Template for Submission of Manuscripts to American Chemical Society Journals

Word 2000, Version 2 (Revised November 2001)

This template is to be used to prepare manuscripts for submission to any American Chemical Society (ACS) primary research journal. As a result, it contains paragraph styles that may not normally be used in the journal you have selected for submission. Please consult the Instructions to Authors or a recent issue of the ACS journal where you plan to submit this paper for the appropriate paragraph styles. Use of this template is a benefit to the author in that the entire manuscript (text, tables, and graphics) may be submitted in one file. Inserting graphics and tables close to the point at which they are discussed in the text of the manuscript can also be a benefit for the reviewer. Use of the template is not a requirement for submission.

When you submit a manuscript using this template, you will not actually see the page formatting that appears in the printed journal. This will occur as part of the editorial production process using the paragraph tags you inserted from the template. Please read the general instructions given below on how to use the template. If you are unfamiliar with the use of templates, additional instructions can be found at the site where you downloaded this template.

Using the template

1. Abbreviated instructions for using the template follow. Additional instructions can be found in the readme file at the site where you downloaded this template.

2. If typing your manuscript directly into the template, select (highlight) the text of the template that you want to replace and begin typing your manuscript (i.e., the select the Title section for typing in your title).

3. If you have already prepared your document in a Word file, you will need to attach the template to your working document in order to apply the Word Style tags. Further instructions can be found in the readme file at the site where you downloaded this template.

   a. Go to the Word Style list on the formatting toolbar and you will see all the Word Styles from the template that have now been imported into the current document. A Styles toolbar has been generated that will display the different Styles for you to choose from. If this is not present, select **View**, **Toolbars**, and then select **Styles** and it should appear. You can close this at any time and then reopen it when needed.

   b. Click in the sentence or paragraph and then go to the Word Style menu on the toolbar and select the relevant Word Style. This will apply the Word Style to the entire text (sentence or paragraph). Do this for all sections of the manuscript.

4. In ACS publications there are many different components of a manuscript (i.e., title, abstract, main text, figure captions, etc.) that are represented in the template. See the Guide, Notes, Notice, or Instructions for Authors that appear in each publication's first issue of the year and the journal's homepage to determine which parts should be included for the manuscript that you are preparing.

5. To insert graphics within the text or as a figure, chart, scheme, or table, create a new line and insert the graphic where desired. If your graphic is not visible, ensure that the Word Style is "Normal" with an automatic height adjustment. If the size of the artwork needs to be adjusted, re-size the artwork in your graphics program and re-paste the artwork into the template (maximum width for single-column artwork, 3.3 in. (8.5 cm); maximum width for double-column artwork, 7 in. (17.8 cm)). **NOTE**: If you are submitting your paper to a journal that requires a Table of Contents graphic, please insert the graphic at the end of the file.

6. Delete all sections from the template that are not needed, including these instructions.

7. Save the file with the graphics in place: select **Save As** (**File** menu) and save it as a document file (.doc).

8. Proof a printout of the manuscript (from a 600 dpi or higher laser printer) to ensure that all parts of the manuscript are present and clearly legible.

9. Consult the Info for authors page from the home page of the ACS journal that you have selected for the latest instructions on how to proceed with the submission of your manuscript.

10. Ensure that page numbers are present on all pages before submitting your manuscript.

Modulation of Cellular Apoptosis with Apaf-1 Inhibitors

L. Mondragón,[†] M. Orzáez,[†] G. Sanclimens,[‡] A. Moure,[‡] A. Armiñán,[§] P. Sepúlveda,[£] A. Messeguer[‡], M. J. Vicent*[†] and E. Pérez-Payá*[†,#]

Dept. Medicinal Chemistry. Centro de Investigación Príncipe Felipe, Valencia, Spain. Dept. of Biological Organic Chemistry, IIQAB, CSIC, Barcelona, Spain. Cardioregeneration Unit, Centro de Investigación Príncipe Felipe, Valencia, Spain. Fundación Hospital General Universitario de Valencia, Consorcio Hospital General Universitario de Valencia, Valencia, Spain. Instituto de Biomedicina de Valencia, CSIC, Valencia, Spain.

E-mail: mjvicent@cipf.es and eperez@cipf.es

RECEIVED DATE (to be automatically inserted after your manuscript is accepted if required according to the journal that you are submitting your paper to)

Running Title: Inhibiting apoptosis with Apaf-1 inhibitors.

*To whom correspondence should be addressed. Address: Centro de Investigación Príncipe Felipe. Av. Autopista del Saler, 16. E-46013 Valencia, Spain. Phone: +34-963289680; Fax: +34-963289701; E-mail: mjvicent@cipf.es and eperez@cipf.es

[†] Dept. Medicinal Chemistry. Centro de Investigación Príncipe Felipe, E-46013 Valencia, Spain
[‡] Dept. of Biological Organic Chemistry, IIQAB, CSIC, E-08034 Barcelona, Spain
[§] Cardioregeneration Unit, Centro de Investigación Príncipe Felipe, E-46013 Valencia, Spain
[£] Fundación Hospital General Universitario de Valencia, Consorcio Hospital General Universitario de Valencia, E-46018 Valencia, Spain
[#] Instituto de Biomedicina de Valencia, CSIC. E-46010 Valencia, Spain.

Abbreviations: Apaf-1, apoptotic protease-activating factor; DEVDase, hydrolysis of Ac-DEVD-afc peptide; DTT, dithiothreitol; FCS, fetal-calf serum; MEFs, mouse embryo fibroblasts; MMP, mitochondrial membrane potential; MTT, 3-(4,5-dimethylthiazol-2-yl)-2,5-diphenyltetrazolium bromide; Ni-NTA, (Ni^{2+}-nitrilotriacetate)–agarose; PBS, phosphate buffered saline; PGA, poly-(L-glutamic acid); rApaf-1, recombinant Apaf-1.

ABSTRACT

The programmed cell death or apoptosis plays both physiological and pathological roles in biology. Anomalous activation of apoptosis has been associated with malignancies. The intrinsic mitochondrial pathway of activation of apoptosis occurs through a multiprotein complex named the apoptosome. We have discovered molecules that bind to a central protein component of the apoptosome, Apaf-1, and inhibits its activity. These new first-in-class apoptosome inhibitors have been further improved by modifications directed to improve their cellular penetration to yield compounds that decrease cell death, both in cellular models of apoptosis and in neonatal rat cardiomyocytes under hypoxic conditions.

2

BRIEFS. Inhibiting apoptosis with Apaf-1 inhibitors

Introduction

Apoptosis is a fundamental mechanism of programmed cell death that is regulated physiologically and genetically and plays a central role in development, normal cell turnover and immune system function. Moreover, abnormal apoptotic processes are important and influence the severity of disease progression in a number of pathologies. Defects in appropriate suppression of apoptosis are observed in cancer pathogenesis[1] and autoimmune disorders,[2] while anomalous induced apoptosis plays an important role in acquired immunodeficiency disease (AIDS)[3], neurodegenerative and heart diseases.[4,5] The mechanism of apoptosis is executed by a family of highly conserved proteases known as caspases,[6] which in a cascade of sequential initiator and effector members dismantle the cell. Different cell death stimuli can initiate the mechanism. In particular, defined apoptotic signals activate the mitochondria-mediated or intrinsic pathway that utilizes caspase-9 as its initiator. Caspase-9 activation is triggered by the release to the cytoplasm of proapoptotic proteins from the mitochondrial inter-membrane space, in particular cytochrome c and Smac/Diablo.[7,8] The formation of the macromolecular complex named apoptosome is a key event in this pathway. The apoptosome is a holoenzyme multiprotein complex formed by cytochrome c-activated Apaf-1 (apoptosis protease-activating factor), dATP and procaspase-9. Understanding the mechanisms of functional activation of the apoptosome has helped to define prospective targets for treating deregulated apoptosis that is associated with human pathologies.[9] However, inappropriate apoptosome activity has been shown to play a role in neurodegenerative disorders and its suppression by biological tools provided resistance to apoptosis induction.[10,11] Inactivation of the apoptosome might provide a therapeutic avenue for treating not only neurodegenerative but other diseases as ischemia, cardiac and renal failure.

We have early developed a new structural class of Apaf-1 ligands as apoptosome inhibitors.[12] From this family of *N*-alkylglycine inhibitors the most potent *in vitro* was peptoid **1** (Scheme 1). However this hit exhibited low membrane permeability and modest efficacy arresting apoptosis in cells. We have shown that fusion of peptoid **1** to known cell penetrating peptides[13] facilitates cell permeation in defined cellular models of apoptosis. Furthermore, the conjugation of peptoid **1** to a polymeric carrier (PGA-**1**) demonstrated an enhanced efficacy probably related to an efficient lysosomotropic drug release on the cytosol.[14] Here, we have extended these studies by exploring the activity of PGA-**1** in different cellular models of apoptosis, such as: human cervix adenocarcinoma (HeLa), human histiocytic lymphoma (U937), human osteosarcoma (U2-OS), human lung carcinoma (A549), and human osteogenic Sarcoma (Saos-2) with inducible expression of Bax. In addition, we have also explored how restriction of the conformational mobility of peptoid **1** through backbone cyclization decreased the unspecific toxicity of **1** and increased its antiapoptotic activity. A systematic comparative study of these new first-in-class apoptosome inhibitors has been developed and the results suggested that inhibition of the apoptosome resulted in increased cell recovery, when compared to control cells, after the apoptotic insult. Finally, we carried out studies directed to explore the use of apoptosome inhibitors as agents that could decrease the degree of apoptosis in neonatal rat cardiomyocytes subjected to hypoxic conditions.

Results and Discussion.

To increase the cellular activity of the originally identified apoptosome inhibitor peptoid **1**,[12] structural modifications of this compound had to be done due to its poor solubility and low membrane permeability. The potential production of undesirable side effects due to the conformational freedom of peptoids was also matter of concern. Thus, we focused our studies on delivery systems by means of adequate carriers or on chemical modifications that could diminish the conformational mobility of peptoid **1**. These goals could be addressed in three different ways; (i) by the design of hybrid

peptide/peptoid conjugates where the parent peptoid **1** was fused to well characterized cell penetrating peptides (CPPs) such as penetratin (PEN) and Tat HIV-1 (TAT) peptides, yielding compounds PEN-**1** and TAT-**1**,[13] respectively, (ii) by means of backbone cyclization or (iii) by conjugation to a water soluble polymeric carrier such as poly-L-glutamic acid (PGA) obtaining PGA-peptoid conjugates.[14]
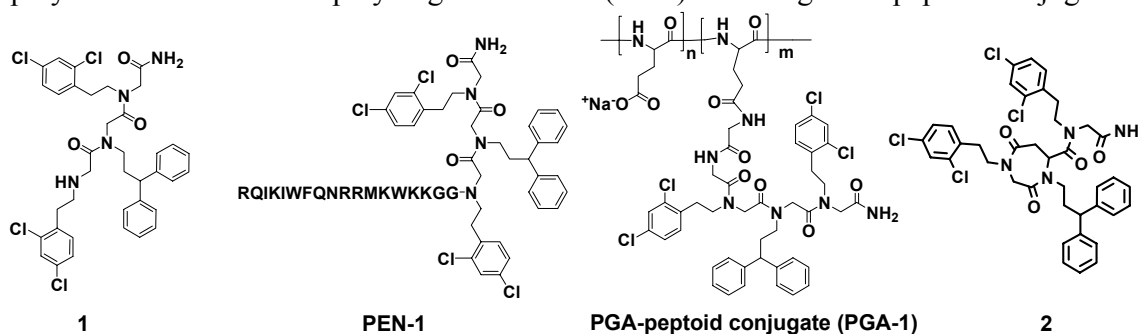
Scheme 1. Chemical structure of **1** and its derivatives studied here. Namely, peptide-peptoid hybrids (as example PEN-**1**; one letter code for the amino acids has been used to describe the peptidic part of the molecule), PGA-peptoid conjugate and the cyclic derivative, **2**.

Cytotoxicity and cell recovery capability of peptoid 1 derivatives. Before proceeding with cellular models of apoptosis inhibition, the unspecific toxicity of the compounds in our cell panel was analyzed by means of MTT assays (see Experimental Section for full details on cell lines) (Figure 1A).

A.   **B.**
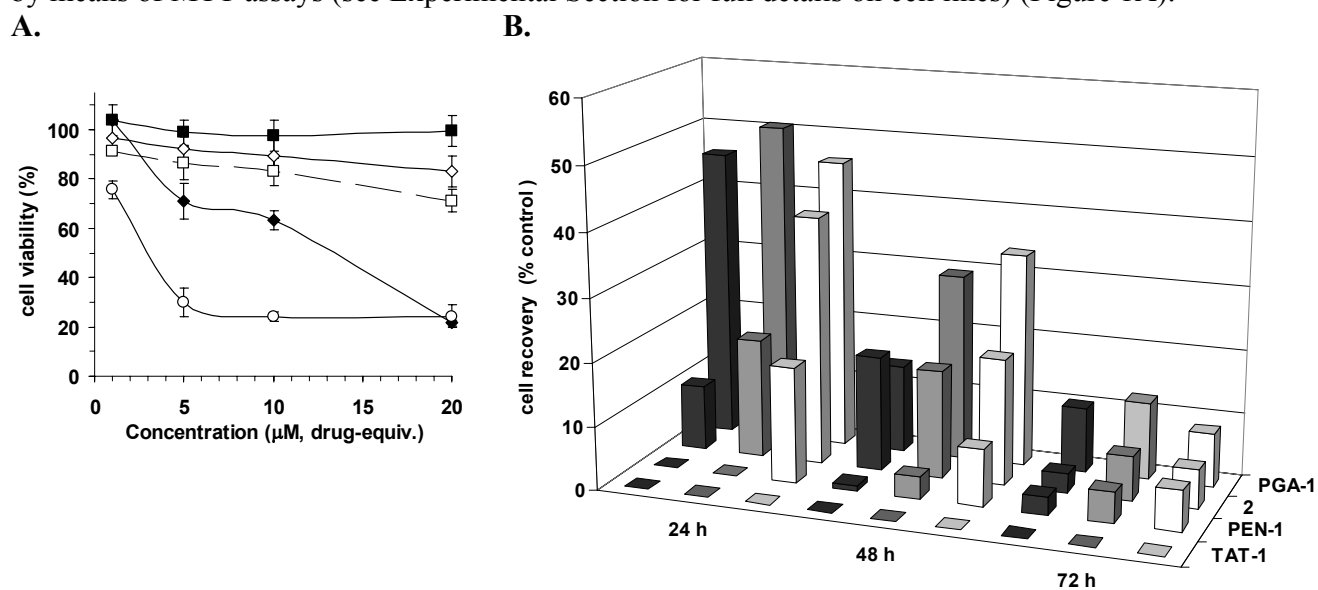
Figure 1. MTT cell viability measurements of peptoid **1** derivatives. Panel A. Cytotoxicity of peptoid **1** (◆), the different peptide/peptoid hybrids (□ PEN-**1** and ○ TAT-**1**), compound **2** (◇) and PGA-**1** (■) against U937 cells measured after 24 h of incubation. Data expressed as mean ± SD (n>3). Panel B. Evaluation of compound-dependent cell recovery after doxorubicin-induced cell death in U2-OS cells. The peptoid derivatives and compound **2** were evaluated at different concentrations (10, 5 and 1 μM (black, grey and white bars, respectively)) after 24, 48 and 72 h of incubation. In all cases SD < 10%. Data expressed as mean ± SD (n>3).

TAT-**1** and PEN-**1** were found to be highly and slightly toxic, respectively, for the cells. In contrast, both **2** and PGA-**1** showed to be devoid of unspecific cell toxicity. The enhancement of peptoid **1**

cytotoxicity after fusion with TAT peptide could be related to a cargo-induced restriction of the conformational space available for the CPPs that could be necessary for an effective and safe cellular membrane permeation.[13] A preliminary analysis of the antiapoptotic activity of peptoid **1** derivatives was performed in osteosarcoma U2-OS cells where the cytotoxic compound doxorubicin induces cell death in a time and concentration dependent manner. Doxorubicin induces apoptosis through DNA damage that is transduced to the mitochondria disturbing the mitochondrial membrane potential (MMP) and activating executioner caspases through involvement of the apoptosome. After 12 h, 2 μM doxorubicin-treated cells demonstrated staining for annexin V-PE (that specifically binds to exposed phosphatidylserine) and lost of MMP, being both features markers of an apoptotic cellular phenotype.[12] When cells were treated with doxorubicin in the presence of **2** and PGA-**1**, the extent of apoptosis was remarkably diminished as determined by the lowered percentage of cells showing apoptotic phenotype (Figure 1B). In contrast, as expected from the previous unspecific cell toxicity evaluation, TAT-**1** did not prevent cellular death and PEN-**1** showed only partial protection at low concentration evidencing a compromise between the protective effect of the peptoid **1** and residual unspecific toxicity associated to the whole molecule (Figure 1B). Compound **2** and PGA-**1** were then selected for a systematic study as cell death inhibitors using different cell lines and different cell death inducers.

To probe the extent of protection against apoptosis of compounds **2** and PGA-**1**, they were evaluated in a panel of different cell models (U937 histiocytic lymphoma, A549 lung carcinoma, HeLa adenocarcinoma and U2-OS osteosarcoma) using doxorubicin as apoptosis inducer. In addition, we also evaluated a more well defined model of 'only intrinsic' apoptosis using Saos-2 cells were apoptosis is induced by the doxycyclin-dependent conditional expression of Bax through the tet-ON system (Clontech). Bax is a pro-apoptotic member of the Bcl-2 family that induces apoptosis through the release of cytochrome *c* from the mitochondria [15,16] thus activation of apoptosis solely relies on the mitochondrial pathway. Figure 2 summarizes the cell death inhibitory activity of **2** (Figure 2A) and PGA-**1** (Figure 2B) in the above-mentioned cell panel.

A.
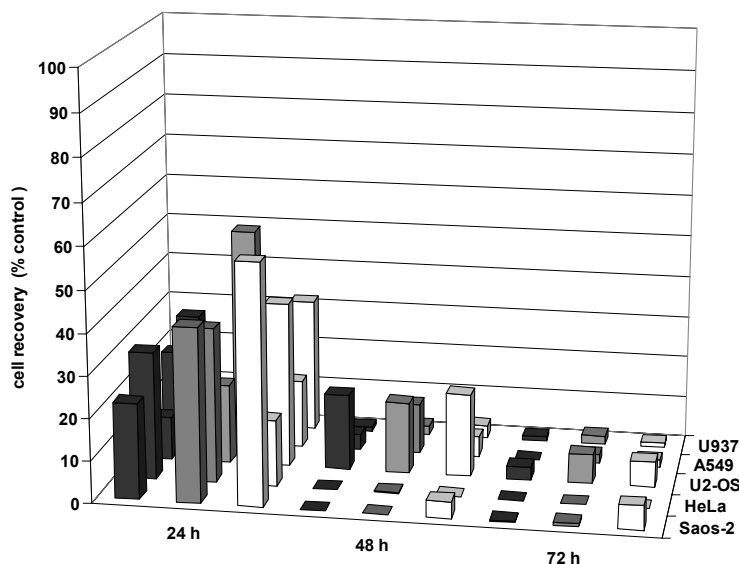
B.
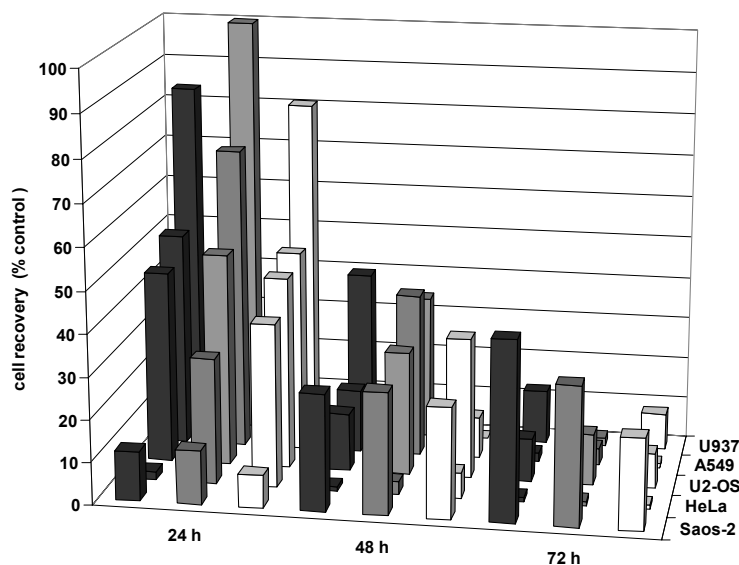
Figure 2. Evaluation of cell death inhibition in different cell lines by **2** (Panel A) and PGA-**1** (Panel B). **2** was evaluated at 10, 5 and 1 μM (black, grey and white bars, respectively) and PGA-**1** at 100, 50 and 20 μM, drug-equiv. (black, grey and white bars, respectively) after 24, 48 and 72 h incubation. Data expressed as mean ± SD (n>3). In all cases SD < 10%.

The two compounds, **2** and PGA-**1** substantially decreased apoptosis in both, doxorubicin-induced (U937, U2-OS, HeLa and A549 cell lines) and doxycyclin-induced (Saos-2 cells) cell death when cell viability was evaluated at 24 h post-treatment (up to 60 percent of cell death inhibition in the Saos-2 cell line was obtained when using a 1 μM concentration of **2** (p<0.001) and up to 100 percent in the U937 cell line when a 50 μM concentration drug-equiv. of PGA-**1** was used (p<0.05). It is important to note that PGA conjugates (i.e. like the PGA-**1** analyzed in the present study) are usually active at concentrations ten fold higher than the parent low molecular weight drugs, due to the different pharmacokinetics.[17]

It is well established that inhibition of apoptotic cell death should correlate with inhibition of executioner caspases. Then, we were willing to evaluate caspase-3 activity in extracts derived from cells that were treated with both, the apoptosis inducer and the inhibitors and compare the results to those obtained from cell extracts only treated with the inducers (Figure 3). Initially, the compounds PEN-**1**, **2** and PGA-**1** were evaluated in a common cell line, Saos-2. At this point, for comparative purposes, we decided to include in our study the diarylurea-based compound **3** previously described as apoptosome inhibitor.[18] PEN-**1** and **3** showed low caspase-3 inhibitory activity in these experimental conditions. However, the inhibition of the apoptosome activity by the treatment of the cells with **2** and PGA-**1**, resulted in inhibition of caspase-3 activity. **2** was effective when the cell extract was obtained after 24 h of treatment while PGA-**1** showed increased activity at longer times (p<0.001) (Figure 3A). The delay on time to reach the activity obtained for PGA-**1** when compared to **2** is probably due to the mechanism of action and cellular pharmacokinetics of polymeric drugs. Effective biological activity of polymer-drug conjugates relies on lysosomal enzyme cleavage to release active drug in a specific place after cellular uptake by endocytosis.[14] Interestingly, PGA-**1** reaches values up to 100 percent of caspase-3 inhibition at 50 μM, drug-equiv. (HeLa at 48 h and Saos-2 at 72 h) (p<0.05) (Figure 3B), whereas **2** at 5 μM reaches inhibitory percentages of 50 to 60 % (U2-OS at 48 h and HeLa at 48h, respectively) (p<0.05) (Figure 3C). The good correlation found in our analysis of caspase-3 inhibition and cell recovery could suggest that the compounds are direct inhibitors of the enzymatic activity of caspase-3, however this is not the case. In fact, none of the compounds here analyzed was able to inhibit caspase-3 using a recombinant-protein based assay (results not shown). In contrast, when we

6

directly activated the apoptosome with an apoptosome activator (compound **4**) recently described by Nguyen and Wells[19], we obtained cell protection when **4** was provided to the cells in the presence of the apoptosome inhibitor PGA-**1** (p<0.001) (Figure3D).

A.
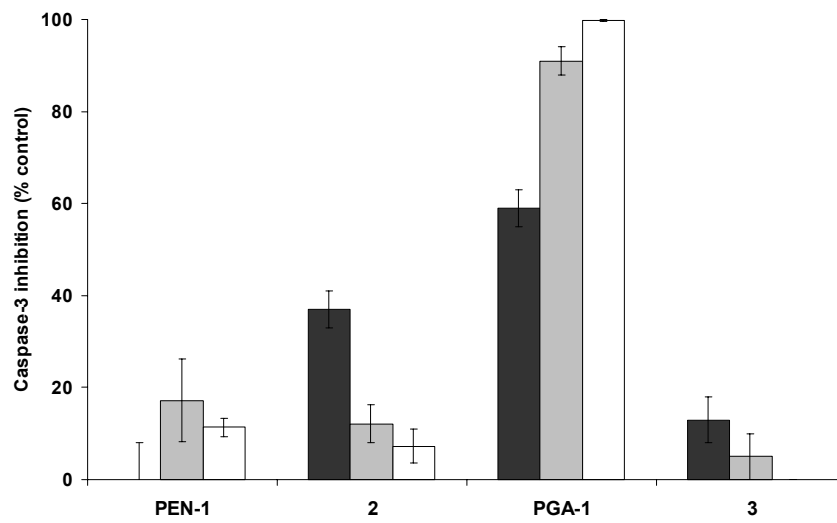
B.
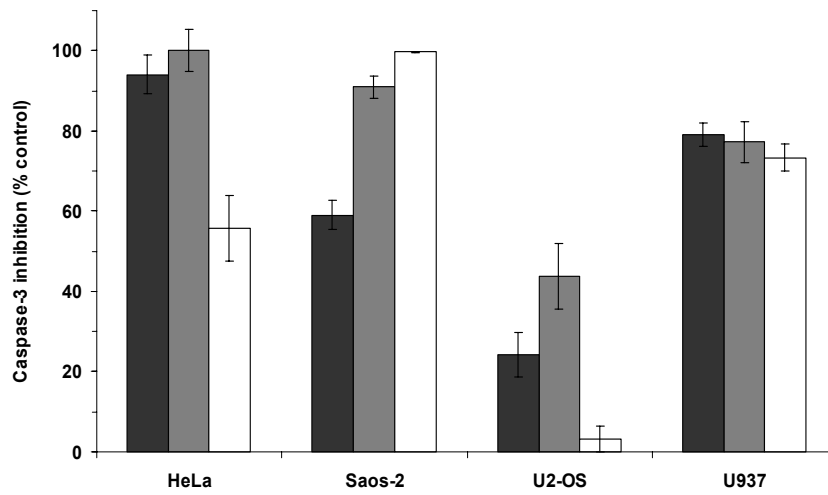
C.
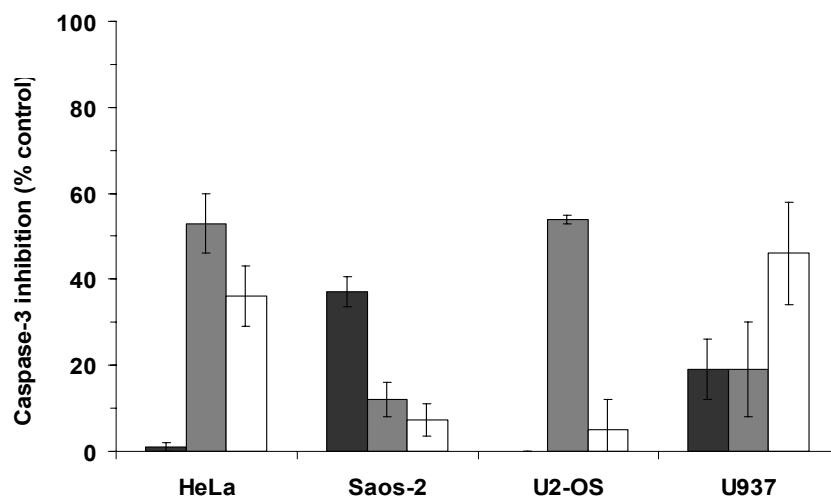
D.
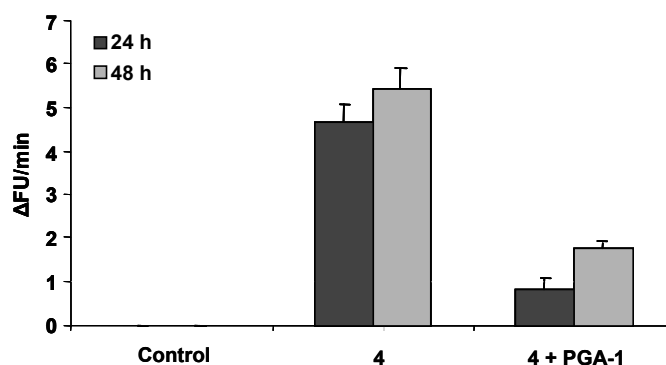
Figure 3. Caspase-3 (C3) activity in cell extracts measured by the fluorimetric DEVDase assay at 24, 48 and 72 h incubation times (black, grey and white bars, respectively). Panel A: Comparison of C3 activity in Saos-2 cell extracts after incubation with the different peptoid **1** derivatives (all compounds at 5 μM concentration except PGA-**1** that was used at 50 μM, drug-equiv). C3 activity in different cell lines after incubation with: PGA-**1** at 50 μM, drug-equiv. (panel B) and **2** at 5 μM concentration (panel C). Panel D: C3 activity in U-937 cells after direct activation of the apoptosome assembly[19] with compound **4** in presence and absence of PGA-**1** at 50 μM, drug-equiv. Data expressed as mean ± SD (n>3).

Compound 2 analogues. As explained above, the cyclic derivative **2** was one of the most active peptoid **1** derivatives together with PGA-**1** conjugate. In order to seek for further optimization, several structural modifications of **2** were carried out. Initially we focused our attention to the 2',4'-dichloro-phenylethyl substituent attached to the perhydro-1,4-diazepine-2,5-dione ring (I, Scheme 2). This substituent turned out to be essential for activity and in our hands, any attempt of modification resulted in a loss of antiapoptotic activity. Similar results were found in early attempts of modification of the 3,3-diphenylpropyl moiety[12]. Then we addressed our attention to the R_1 moiety. As shown in Table 1, a series of 8 derivatives (**2a-2h**) were designed and their preparation was carried out by using a practical approach. Thus, according both to the nature of the R_1 moiety and to the expected behavior of the mixtures in preparative HPLC, these analogues were separated into three subsets containing 2, 3 and 3 compounds (**2a** and **2b**, **2c-2e** and **2f-2h**), respectively. Then each subset of compounds was prepared by using a synthetic pathway based on solid-phase and microwave activation and using the positional scanning approach for construction of controlled mixtures. By this procedure, three HPLC purifications were only required for isolating all compounds in purities over 98% and satisfactory overall yields.
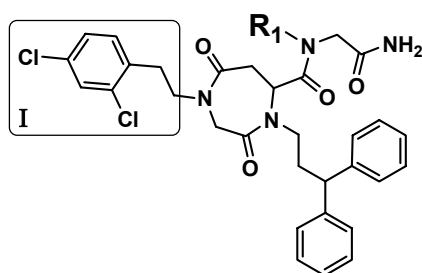
Scheme 2. Chemical structure of **2** and its derivatives here studied.

Table 1. Percentage of cell recovery and inhibition of caspase-3 activity obtained with compound **2** analogues in Bax-induced apoptosis in Saos-2 cell line[a].

Compound 2 analogues	R_1	Cell recovery assay (%)[a]	Caspase-3 inhibition assay (%)[a]
2		50 ± 3	53 ± 4
2a		57 ± 18	34 ± 8
2b		10 ± 6	16 ± 11
2c		2 ± 1	45 ± 5
2d		9 ± 5	ND
2e		16 ± 8	51 ± 5
2f		12 ± 6	21 ± 9
2g		41 ± 12	1 ± 1
2h		23 ± 10	2 ± 1

ND: not determined. [a] Cell recovery and caspase-3 activity were analyzed after 24 h of treatment with the respective compounds at 5 μM concentration. Data expressed as mean ± SD (n>3).

Table 1 summarizes the caspase-3 inhibitory activity determined in cell extracts and the observed cell recovery when apoptosis was induced in Saos-2 cells upon treatment with doxycyclin, in the presence or absence of the compound subjected to evaluation. As expected from previous results, replacement of the 2',4'-dichlorophenylethyl moiety at R_1 by a non-aromatic moiety resulted in a decrease of potency (compounds **2c**, **2d**, **2e**, **2g**). However, the behavior of compound **2c** was a bit aside provided that the

inhibition of caspase-3 activity was systematically close to 50 % while the cell recovery ability was 2 %. Also, the activity in the cell recovery experiment for this compound was slightly higher at 1 μM (not shown) than at 5 μM. It should be mentioned that in certain occasions, biological assays developed with cell extracts and whole cell systems provide results which are more difficult to rationalize when compared to those obtained from *in vitro* experiments. Furthermore, parallel studies addressed to analyze the unspecific toxicity of the compounds, suggested that only compound **2d** was toxic. Different electronegative atoms (such as O or F) in several positions (*p-, m-* or *o-*) were also used in order to evaluate the effect of the electronic density changes on this family of apoptosome inhibitors (namely, **2a**, **2e**, **2g** and **2h**). In general, although all these analogues exhibited capability to reduce the apoptosis induced in Saos-2 cell line, none of them showed a significant improvement when compared to compound **2**. Similar results were obtained in the other models of our cell panel mentioned above (HeLa, A549, U2-OS and U-937 cells, data not shown). Taken all together, it is not easy to make an appropriate SAR as no clear trend was obtained. However, it would be possible to suggest that the presence of a second 2',4'-dichlorophenylethyl substituent is not essential but important for the activity, probably due to the presence of the two electronegative atoms and, certainly, of the aromatic ring. This is still an ongoing research and new efforts are currently being devoted to modify either the 1,3-diphenylpropyl substituent as well as to explore other heterocyclic scaffolds.

Membrane potential recovery after PGA-1 treatment. Mitochondria play a prominent role in cell death as a central organelle involved in the signal transduction and amplification of the apoptotic response.[20,21] Mitochondrial dysfunction is an early event characterized by an increase in mitochondrial membrane permeability. Thus, cells undergoing apoptosis are characterized by a low mitochondrial membrane potential ($\Delta\Psi_m^{low}$). In fact, when Saos-2 and U937 cells were subjected to an apoptotic insult (Saos-2 treated with doxycycline and U937 with doxorubicin) the number of cells with $\Delta\Psi_m^{low}$ increased when compared to untreated cells ($p<0.05$) (Figure 4). However, the effect was clearly attenuated when cells were subjected to the insult in the presence of PGA-**1**. This result suggests that PGA-**1**-treated cells could probably overcome apoptosis at this post-mitochondrial level of the pathway. Although still speculative, this class of compounds could inhibit processes downstream the mitochondrial depolarization event. Then, damaged cells, at early stages of depolarization, could still be in a reversible step of the apoptotic process, and inhibition of Apaf-1 could result in a recovery of mitochondrial potential. Another possibility is that the recovery of membrane potential of the population would be related to a process downstream the mitochondria, such as the loss or not of plasmatic membrane potential caused by a decrease in the intracellular levels of K^+ ions. Although the ability of mitochondrial recovery after partial depolarization is still a matter of discussion, it seems well accepted that it could occur in neurons [22] but it is controversial in other cell types as smooth muscle cells or myofibroblasts[23].
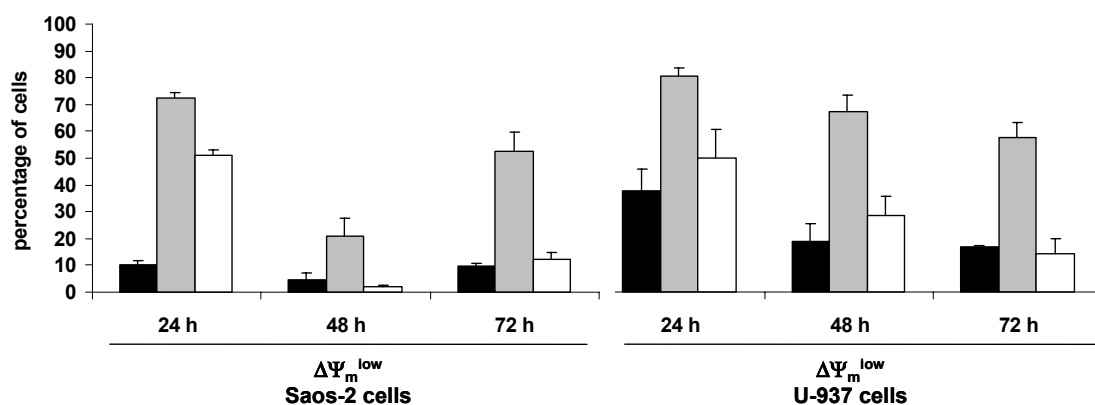
Figure 4. Evaluation of apoptosis by flow cytometry as the percentage of cells with low membrane potential ($\Delta\Psi_m^{low}$). Flow cytometry analysis of $\Delta\Psi_m$ of Saos-2 and U-937 cells untreated (black bars);

subjected, respectively, to an apoptotic insult by treatment with doxycyclin and doxorubicin, respectively (grey bars); and when the apoptotic insult was applied in the presence of PGA-**1** at 50 μM, drug-equiv. (white bars). Data expressed as mean ± SE (n>3).

Inhibition of hypoxia-induced apoptosis in primary culture cardiomyocytes by PGA-1. Apoptosis plays a crucial role in ischemic-based diseases. Among them, myocardial damage induced by ischemia-reperfusion has been shown to be directly associated to apoptosis. Furthermore, after myocardial infarction, the presence of apoptotic cells has been demonstrated both in the infarct area and in the border zone of the infarction[24-29]. Although the signal transduction pathways are not completely defined, it is known that mitochondrial dysfunction is one of the most critical events associated with myocardial ischemia-reperfusion injury[30,31]. In this sense, previous studies showed that very low levels of cardiac myocyte apoptosis are sufficient to produce heart failure[32]. In addition, reduction of myocyte apoptosis by the potent polycaspase inhibitor IDN-1965, improved left ventricular function and survival of mice with an induced peripartum cardiomyopathy[33]. We therefore analyzed the ability of the apoptosome inhibitors here described, and in particular PGA-**1**, as a potential inhibitor of hypoxia-induced apoptosis in cardiomyocytes as an *ex-vivo* model of myocardial infarction. Then, primary cultures of neonatal rat cardiomyocytes were established and subjected to hypoxic conditions. A double immunohistochemistry-based procedure clearly showed the presence of apoptotic cells and active caspase-3 demonstrating the active role of apoptosis in hypoxia-induced cardiomyocytes cell death (Figure 5A). The presence of Apaf-1 protein in neonatal cardiomyocytes was also determined by western blot (data not shown). These results provide a validation of the cellular model selected for our *ex-vivo* studies. Importantly, when the neonatal cardiomyocytes were subjected to the hypoxia conditions in the presence of PGA-**1**, the percentage of cell death was clearly diminished when compared to the control cell population ($p<0.05$) (Figure5B). Furthermore, to determine whether or not PGA-**1** could decrease caspase-3 activity in this cell system, cells from a 2-days old established culture were subjected to the hypoxia conditions in the presence of different concentrations of PGA-**1** and caspase-3 activity was assessed (Figure 5C). The results revealed a marked PGA-**1**-dependent decrease of caspase-3 activity ($p<0.001$).
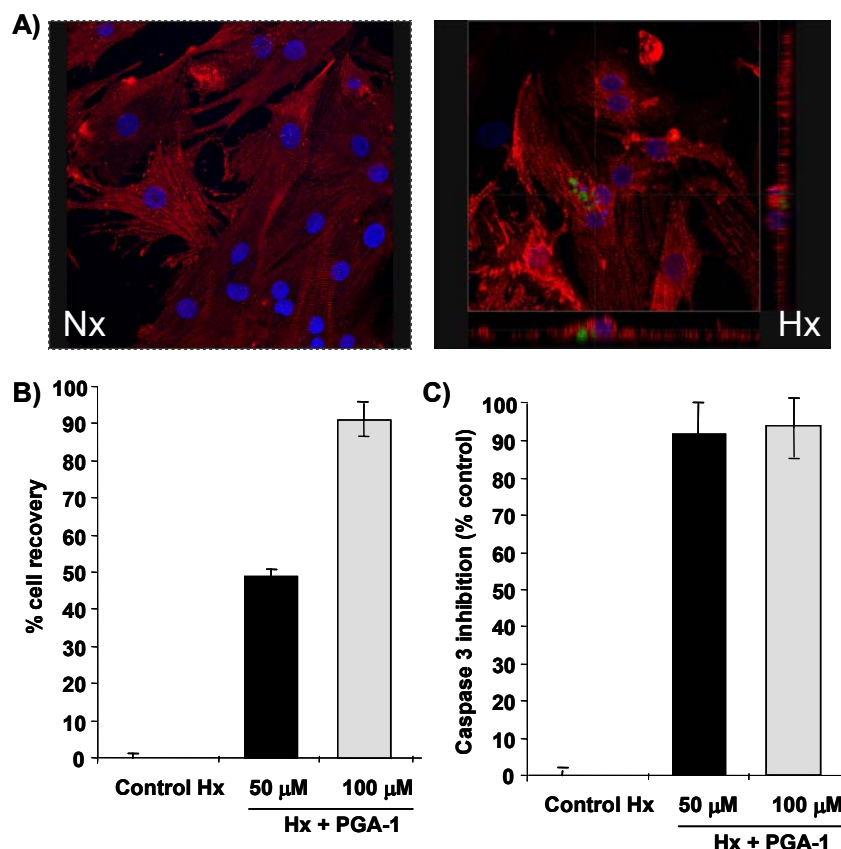
Figure 5. PGA-**1** is capable to reduce hypoxia-induced apoptosis in primary culture cardiomyocytes. Panel A: Apoptosis induction in primary culture cardiomyocytes subjected to hypoxia. Double immunohistochemistry of cardiomyocytes with anti-caspase 3 (green) and anti-α-Actinine (red) antibodies analyzed by confocal microscopy. (40x magnification). Nucleus are stained with DAPI (blue). Panel B: Evaluation of induced cell death inhibition by MTT assay. PGA-**1** at different concentrations (50 and 100 μM drug-equiv.; black and grey, respectively) after 24 h incubation. Panel C: Caspase-3 activity in cell extracts measured by the fluorimetric DEVDase assay at 24 h incubation time. Data expressed as mean ± SE (n>3).

Conclusions.

   The overall data obtained suggest that apoptosome inhibitors can decrease the extension of cell death. Two important concepts come into view from this study. First, compound **2** and the PGA-based derivative PGA-**1** inhibit apoptosis in different cell lines. Second, inhibition of the intrinsic cell death (or mitochondrial) pathway by specific inhibition of Apaf-1 could result in the recovery of the cells or in prevention of the cellular damage induced by apoptotic insults. Whether or not this could have therapeutic interest is a fundamental question. In this sense, we have observed that PGA-**1** was active inhibiting hypoxia-induced cell death in cardiomyocytes. Although the results shown here are derived from *ex-vivo* studies, we are now moving ahead to the next level of complexity that represents an appropriate *in vivo* model. We are currently evaluating different experimental models of myocardial infarction. If the compounds here analyzed further demonstrate to be able to reduce hypoxia-induced cardiomyocyte apoptosis *in vivo*, it would result in a prevention of ventricular remodelling and improvement of damaged cardiac function. That, in turn, would open new strategies to improve the therapeutic resources for the treatment of this, unfortunately, very common pathology.

Experimental Section

Materials. Poly-L-glutamic acid sodium salt (PGA), *N,N*-Diisopropylcarbodiimide (DIC), 1-hydroxybenzotriazole (HOBt), diisopropylethylamine (DIEA) and anhydrous dimethylformamide (DMF) were purchased from Sigma-Aldrich and used without further purification. All solvents including HPLC grade were obtained from Merck (Barcelona, Spain). Tissue culture grade dimethylsulfoxide (DMSO), 3-(4,5-dimethylthiazol-2-yl)-2,5-diphenyl tetrazolium bromide (MTT), trypan blue solution (0.4%) (cell culture grade), bovine cathepsin B and dithiothreitol (DTT) were from Sigma-Aldrich. 0.25 % Trypsin-EDTA, fetal calf serum (FCS), RPMI 1640, with L-glutamine, D-MEM with L-glutamine and collagenase Type II were from Gibco BRL Life Technologies (Paisley, UK). Annexin V-FITC Apoptosis detection kit I was from BD PharmingenTM (BD Bioscience, Madrid, Spain) and 3,3'-dihexyloxacarbocyanine iodide ($DIOC_6(3)$) from Molecular Probes (Invitrogen, Barcelona, Spain). The fluorogenic caspase 3 substrate, Ac-DEVD-afc, was purchased from Biomol International LP (Exeter, UK). Protein quantification was performed with a bicinchoninic acid kit from Pierce Technology Corporation (New Jersey, USA). Dispase was purchased from Roche Diagnostics (Godo Shusei Co, Ltd, Tokyo, Japan). For immunochemistry assays, rabbit polyclonal active caspase-3 antibody was purchased from Cell Signalling Technology (Beverly, MA, USA) and mouse monoclonal anti- α-actinine (Sarcomeric) was purchased from Sigma-Aldrich. Anti-rabbit and anti-mouse secondary antibodies were coupled to FITC and cyanine-3, respectively, and were purchased from Jackson Immunoresearch (Suffolk, England). All other reagents were of general laboratory grade.

Chemistry. The HPLC analyses of peptoid **1** and compound **2** and its analogs were carried out with a Hewlett Packard Series 1100 (UV detector 1315A) modular system using a Kromasil 100 C8 (15 x 0.46 cm, 5 μm) column, with CH_3CN-H_2O mixtures containing 0.1 % TFA at 1 mL/min as mobile phase and monitoring at 220 nm. Compounds were purified from the crude reaction mixture by semi-preparative HPLC using a Kromasil C8 (25 x 2 cm, 5 μm) column, CH_3CN-H_2O mixtures containing 0.1 % TFA as mobile phases and a flow rate of at 5 mL/min. The NMR spectra of peptoids were recorded in CD_3OD solutions using a Varian Inova 500 apparatus (^{1}H NMR, 500 MHz; ^{13}C NMR, 125 MHz). The assignments of absorptions observed for peptoid **1** and compound **2** were confirmed by gDQCOSY and gHSQC experiments. The different conformations present in both compounds led to the observation of complex absorptions. High resolution mass spectra (HRMS-FAB) were carried out at the Mass Spectrometry Service of the University of Santiago de Compostela (Spain). The synthesis and characterization of PGA-**1**, PEN-**1** and TAT-**1** have been reported[13,14].

Synthesis of [*N*-(2,4-dichlorophenethyl)glycyl]-[*N*-(3,3-diphenylpropyl)]glycyl]-*N*-(2,4-dichlorophenethyl)glycinamide (1). The synthesis of this peptoid was carried out following the method described elsewhere[34] **1**: ^{1}H-NMR: 7.5-7.4 (2H, CH_{Ar}), 7.25-7.35 (12H, CH_{Ar}), 7.15 (2H, CH_{Ar}), 4.2-3.8 (6H, $COCH_2N$), 4.02 (1H, C̲H̲), 3.58 (2H, NCH_2CH_2), 3.20 (2H, NCH_2CH_2CH), 3.15 (2H, NHC̲H̲$_2$CH$_2$), 3.10 (2H, $NHCH_2CH_2$), 3.0-2.90 (2H, NCH$_2$C̲H̲$_2$), 2.4-2.1 (2H, NCH$_2$C̲H̲$_2$CH); ^{13}C-NMR: 172.62, 172.39 (CO), 170.14, 169.87 (CO), 167.53, 166.60 (CO), 145.85 (2 x C_{Ar}), 136.0 (2 x C_{Ar}), 134.2 (2 x C_{Ar}), 133.8 (2 x C_{Ar}), 133.2, 133.1 (2 x CH_{Ar}), 129.8 (2 x CH_{Ar}), 129.5 (2 x CH_{Ar}), 128.9 (4 x CH_{Ar}), 128.8 (4 x CH_{Ar}), 127.4 (2 x CH_{Ar}), 50.4 ($COCH_2N$), 49.5 (C̲H̲), 49.1 (NCH_2CH_2), 48.9 ($COCH_2N$), 48.2 (NCH_2CH_2CH), 48.1 ($COCH_2N$), 47.8 (HNC̲H̲$_2$CH$_2$), 34.2 (NCH_2CH_2CH), 32.6 (NCH$_2$C̲H̲$_2$), 30.4 (HNCH$_2$C̲H̲$_2$). HRMS (M + 1): Calcd. $C_{37}H_{39}$[35]$Cl_4N_4O_3$: 727.1747, found: 727.1751.

Synthesis of 1-(3',3'-diphenylpropyl)-4-[2'-(2'',4''-dichlorophenyl)ethyl]-7-[*N*-aminocarbonylmethyl-*N*-[2'-(2'',4''-dichlorophenyl)ethyl]aminocarbonyl]perhydro-1,4-diazepine-2,5-dione (2). The synthesis of this heterocyclic derivative was carried out following a solid-phase general procedure with microwave activation developed in our laboratory that is briefly described below for the preparation of compound **2** analogues and that will be reported elsewhere. **2**: ^{1}H-NMR: 7.62-7.53 (2H), 7.48-7.35 (2H), 7.32-7.23 (10H), 7.16 (m, 2H), 4.70, 4.60 (1H, $(CH)_{het}$), 4.21, 4.19 (d, *J*=17.1 Hz, 1H, $(COCH_2N)_{het}$), 4.02-3.78 (1H $(COCH_2N)_{het}$ + 2H ($COCH_2N$) + 1H (CH)), 4.02 (C̲H̲Ph$_2$), 3.53-3.45 (6H, NC̲H̲$_2$CH$_2$), 3.00, 293 (dd, *J*=14.7 and 6.3 Hz, 1H, COC̲H̲$_2$CH), 2.90-2.71 (5H, 1H (COC̲H̲$_2$CH) + 4H(NCH$_2$C̲H̲$_2$)), 2.48-2.15 (2H, NCH$_2$C̲H̲$_2$CH); ^{13}C-NMR: 172.5 (CO), 171.5, 170.8 (CO), 170.1 (CO), 169.3 (CO), 145.4 (C_{Ar}), 145.0 (C_{Ar}), 136.3-135.4 (2 x C_{Ar}), 134.7 (2 x C_{Ar}), 133.5

(CH$_{Ar}$), 133.1 (CH$_{Ar}$), 132.9 (CH$_{Ar}$), 132.5 (2 x C$_{Ar}$), 129.4-129.0 (4 x CH$_{Ar}$), 128.1 (4 x CH$_{Ar}$), 126.8 (CH$_{Ar}$), 126.7 (CH$_{Ar}$), 56.0, 55.6 (CH$_{het}$), 54.2-49.7 (2 x COCH$_2$N), 49.2, 49.0 (CH), 47.8, 47.7 (N$\underline{CH_2}$CH$_2$), 47.0 (N$\underline{CH_2}$CH$_2$), 46.9 (N$\underline{CH_2}$CH$_2$CH), 37.6, 37.1 (CO$\underline{CH_2}$CH), 32.7, 32.5 (NCH$_2$$\underline{CH_2}$CH), 31.4 (NCH$_2$$\underline{CH_2}$), 30.8 (NCH$_2$$\underline{CH_2}$). HRMS (M + 1): Calcd. C$_{39}$H$_{38}$^{35}Cl$_4$N$_4$O$_4$: 767.1720, found: 767.1735.

Synthesis of compound 2 analogues. The preparation of the first set of analogues (**2c**, **2d** and **2e**) was carried out as follows. After all operations carried out in solid phase, the polymer was drained and washed with with DCM (3 x 3 mL) and DMF (3 x 3 mL). Thus, three syringes were prepared with 250 mg of Rink amide resin (0.2 mmol) and treated separately with 3 mL of 20% piperidine in DMF. The resins were filtered and washed. Subsequently, resins were treated with a solution of bromoacetic acid (130 mg, 5 eq.) and DIC (145 µL, 5 eq.) in DMF (3 mL). The reaction mixtures were stirred for 2 min at 60 ºC in a microwave reactor. After draining and washing, a solution of (tetrahydrofuran-2-yl)methanamine (98 µL, 5 eq.) and Et$_3$N (131 µL, 5 eq.) in 3 mL of DMF was added to the first resin and the suspension was stirred for 2 min at 90 ºC under microwave activation. Another solution of butylamine (93 µL, 5 eq.) and Et$_3$N (131 µL, 5 eq.) in 3 mL of DMF was added to the second resin and the suspension was stirred for 2 min at 90 ºC under microwave activation. Finally, the third resin was treated with a solution of 2-(2-fluorophenyl)ethanamine (123 µL, 5 eq.) and Et$_3$N (131 µL, 5 eq.) in 3 mL of DMF and the suspension was stirred for 2 min at 90 ºC under microwave activation. The supernatant of the three resins was removed and the residue was drained and washed. Afterwards, all resins were mixed into the same syringe and the subsequent steps were carried out altogether. The overall resin was treated with a solution of allyl maleate (440 mg, 5 eq.), HOBt (380 mg, 5 eq.) and DIC (436 µL, 5 eq.) in DCM: DMF (2:1, 5 mL). The reaction mixture was stirred at room temperature for 30 min, filtered and the reaction was repeated under the same conditions. After draining and washing the resin, a solution of 3,3-diphenylpropylamine (594 mg, 5 eq.) and Et$_3$N (395 µL, 5 eq.) in 6 mL of DMF was added to the resin and the suspension was stirred for 3 h at room temperature. The reaction was repeated for overnight at the same temperature. The supernatant was removed and the residue was drained and washed. Then, the resin was treated with a solution of bromoacetic acid (391 mg, 5 eq.) and DIC (436 µL, 5 eq.) in DMF (6 mL). The reaction mixture was stirred for 2 min at 60 ºC in a microwave reactor. The resin was drained and washed. A solution of 2,4-dichlorophenethylamine (425 µL, 5 eq.) and Et$_3$N (395 µL, 5 eq.) in 6 mL of DMF was added to the resin and the suspension was stirred for 2 min at 90 ºC under microwave activation. The supernatant was removed, and the residue was drained and washed. Then, the resin was treated with Pd(PPh$_3$)$_4$ (65 mg, 0.1 eq.) and PhSiH$_3$ (693 µL, 10 eq.) in anhydrous DCM for 15 min at room temperature under an inert atmosphere. The supernatant was removed and the residue was drained and washed. The final cyclization was promoted by treatment with PyBOP (440 mg, 1.5 eq.), HOBt (114 mg, 1.5 eq.) and DIEA (300 µL, 3 eq.) in DMF (6 mL). The reaction mixture was stirred at room temperature for 16 h and filtered. Finally, treatment of the resin (1,013 g) with a mixture of 60:40:2 TFA/DCM/water released a crude reaction mixture containing the three target compounds. Solvents from the filtrate were removed by evaporation under reduced pressure followed by lyophilization. The residue obtained (286 mg) was characterized by analytical RP-HPLC and RP-HPLC-MS using aqueous acetonitrile gradient (20% CH$_3$CN → 80% CH$_3$CN, 20 min). Retention times of compounds were found to be 17.14 for **2d**, 18.1 min for **2c** and 19.0 min for **2e**. The crude reaction mixture was purified by semipreparative RP-HPLC using aqueous acetonitrile gradient (42% CH$_3$CN → 80% CH$_3$CN, 35 min) to give the desired products (yield 30 – 47 %, ≥ 98% purity).

1-(3',3'-diphenylpropyl)-4-[2'-(2'',4''-dichlorophenyl)ethyl]-7-[*N*-(aminocarbonylmethyl)-*N*--[(tetrahydrofuran-2'-yl)methyl]aminocarbonyl]perhydro-1,4-diazepine-2,5-dione (2d): HRMS (M + H)$^+$ calcd. for C$_{35}$H$_{40}$^{35}Cl$_2$N$_4$O$_5$, 679.2449. Found 679.2443.

1-(3',3'-diphenylpropyl)-4-[2'-(2'',4''-dichlorophenyl)ethyl]-7-[*N*-(aminocarbonylmethyl)-*N*-(butyl)aminocarbonyl]perhydro-1,4-diazepine-2,5-dione (2c): HRMS (M + H)$^+$ calcd. for C$_{35}$H$_{40}$^{35}Cl$_2$N$_4$O$_4$ 651.2499. Found 651.2524.

1-(3',3'-diphenylpropyl)-4-[2'-(2'',4''-dichlorophenyl)ethyl]-7-[N-(aminocarbonylmethyl)-N-[2'-(2''-fluorophenyl)ethyl]aminocarbonyl]perhydro-1,4-diazepine-2,5-dione (2e): HRMS (M + H)$^+$ calcd. for $C_{39}H_{39}{}^{35}Cl_2FN_4O_4$: 717.2405. Found 717.2396.

The same procedure was carried out for the synthesis of the second and the third subset of compound **2** derivatives (**2f**, **2g** and **2h**) and (**2a** and **2b**), respectively. Retention times for compounds were: 16.49 for **2f**, 20.91 min for **2g** and 21.55 min for **2h**, and 20.58 min for **2b**. The corresponding crude reaction mixtures were purified as described above to yield the expected compounds in 30-45% yields and $\geq$ 98% purity).

1-(3',3'-diphenylpropyl)-4-[2'-(2'',4''-dichlorophenyl)ethyl]-7-[N-(aminocarbonylmethyl)-N-(2'-acetylaminoethyl)aminocarbonyl]perhydro-1,4-diazepine-2,5-dione (2f): HRMS (M + H)$^+$ calcd. for $C_{35}H_{39}{}^{35}Cl_2N_5O_5$ 680.2401. Found 680.2376.

1-(3',3'-diphenylpropyl)-4-[2'-(2'',4''-dichlorophenyl)ethyl]-7-[N-(aminocarbonylmethyl)-N-[2'-(2''-methoxyphenyl)ethyl]aminocarbonyl]perhydro-1,4-diazepine-2,5-dione (2g): HRMS (M + H)$^+$ calcd. for $C_{40}H_{42}{}^{35}Cl_2N_4O_5$ 729.2605. Found 729.2613.

1-(3',3'-diphenylpropyl)-4-[2'-(2'',4''-dichlorophenyl)ethyl]-7-[N-aminocarbonylmethyl-N-[2'-(4''-chlorophenyl)ethyl]aminocarbonyl]perhydro-1,4-diazepine-2,5-dione (2h):. HRMS (M + H)$^+$: calcd. for $C_{39}H_{39}{}^{35}Cl_3N_4O_4$ 733.2110. Found 733.2084.

1-(3',3'-diphenylpropyl)-4-[2'-(2'',4''-dichlorophenyl)ethyl]-7-[N-(aminocarbonylmethyl)-N-(cyclopropyl)aminocarbonyl]perhydro-1,4-diazepine-2,5-dione (2b): HRMS (M + H)$^+$: calcd. for $C_{34}H_{36}{}^{35}Cl_2N_4O_4$ 635.2186. Found 635.2173.

1-(3',3'-diphenylpropyl)-4-[2'-(2'',4''-dichlorophenyl)ethyl]-7-[N-(aminocarbonylmethyl)-N-[2'-(4''-fluorophenyl)ethyl]aminocarbonyl]perhydro-1,4-diazepine-2,5-dione (2a): HRMS (M + H)$^+$: calcd. for $C_{39}H_{39}{}^{35}Cl_2FN_4O_4$ 717.2405. Found 717.2410.

Biological Assays. Cell culture and culture conditions. The U937 human histiocytic lymphoma and the U2-OS human osteosarcoma cell lines were obtained from the American Type Culture Collection (Rockville, MD). The U937 cells were grown in suspension in RPMI 1640 medium supplemented with 10% FCS, and 2 mM L-glutamine. The Saos-2 human osteosarcoma cell line were kindly provided by Karin Vousden (Cancer Research UK, Glasgow) and the HeLa human cervix adenocarcinoma cell lines were kindly provided by Jaime Font de Mora (CIPF, Valencia, Spain). The U2-OS, Saos-2, HeLa and A549 cells were grown in Dulbecco's modified Eagle´s medium supplemented with 15% FCS and 2 mM L-glutamine in all cases except in Saos-2. Cells were maintained at 37 °C in an atmosphere of 5 % carbon dioxide and 95 % air and underwent passage twice weekly.

Culture of neonatal rat cardiomyocytes and hypoxic conditions. Rat neonatal cardiomyocytes were prepared from ventricles of 1-2 days Wistar rats by a previously described method,[33,35] with some modifications. Briefly, hearts were isolated, auricles were discarded and ventricles were minced and digested with 2 mg/ml of collagenase Type II for 1h and subsequently with 1.2 U/ml dispase for 30 min with gently shaking. After two washes primary cultures were pre-plated for 90 min to eliminate contaminating fibroblasts. Hypoxia was induced by incubating the cardiomyocyte cultures in atmosphere of 1 % O_2. Experiment was performed three times with different breedings. Each procedure was repeated twice for two identically treated culture flasks.

MTT cell viability assays[36]. Cells were cultured in sterile 96-well microtitre plates at a seeding density of 10^4, 3 x 10^3, 2.5 x 10^3 and 2 x 10^3 cells/well for Saos-2, U-2 OS, HeLa and A549, respectively, and 2.5 x 10^3 and 4 x 10^3 cells/well in the case of U937, and allowed setting for 24 h. Doxycycline (2 µg/mL in PBS) for Saos-2 cells and doxorubicin in the case of A549, HeLa, U2-OS and U937 at concentrations of 1, 1.5, 2 and 0.25 µg/mL in PBS, respectively; were then added and after 30 min cells were treated with compounds (0.2 µm filter sterilised) at final concentrations of 1, 5 and 10 µM in the case of PEN-**1**, TAT-**1** and **2** and its derivatives, while PGA-**1** was tested at concentrations of 20, 50 and 100 µM, drug equivalents. Compounds were incubated for 19 h, then MTT (20 µL of a 5 mg/mL solution) was added to each well, and cells were further incubated for 5 h (a total of 24 h

15

incubation with the inhibitors was therefore studied). In the next step, medium was removed and the precipitated formazan crystals were dissolved in optical grade DMSO (100 µL), and plates were read at 570 nm using a Wallac 1420 Workstation.

Caspase activation assays in cellular models (DEVDase activity). Cell extracts were prepared from cells seeded in 3.5 cm diameter plates at seeding densities of 2×10^5 cells per plate in the case of Saos-2, 3×10^5 and 3.5×10^5 cells per plate for HeLa and U-2 OS, and 4×10^5 and 4.5×10^5 cells per plate for U937, and allowed setting for 24 hours[12]. Then, cells were treated with doxycycline (2 µg/mL in PBS) for Saos-2 cells and doxorubicin in the case of HeLa, U2-OS and U937 at concentrations of 2, 2.5 and 0.25 µg/mL in PBS, respectively. After 30 minutes, PEN-**1** and compound **2** derivatives at concentrations of 5 µM, and PGA-**1** at concentrations of 50 and 100 µM, drug equivalents were added. Cells were harvested after 24, 48 and 72 h of incubation and pellets re-suspended in 30 µL of extraction buffer (50 mM PIPES, 50 mM KCl, 5 mM EDTA, 2 mM MgCl$_2$, 2 mM DTT supplemented with protease inhibitor cocktail from Sigma) and kept on ice 5 min. Once pellets were frozen and thaw 3 times, cell lysates were centrifuged at 14000 rpm 5 min and supernatants were collected. Quantification of total protein concentration from these cell extracts was performed using the bicinchoninic acid method. Aliquots were prepared at the same concentration and afterwards they were mixed with 200 µL of caspases assay buffer (PBS, 10 % glycerol, 0.1 mM EDTA, 2 mM DTT) containing 20 µM Ac-DEVD-afc. Caspase activity was continuously monitored following the release of fluorescent afc at 37 ºC using a Wallac 1420 Workstation (λexc= 400 nm; λem= 508 nm). DEVDase activity was expressed as the increase of relative fluorescence units per min (ΔFU/min).

Evaluation of cellular apoptosis by flow cytometry analysis. Saos-2 and U937 cells were seeded in 6-well plates at a seeding density of 2×10^5 and 4×10^5 cells per plate, respectively. Cells were treated with doxycycline (2 µg/mL in PBS) and doxycycline plus PGA-**1** (50 µM drug-equiv) for Saos-2 or doxorubicin (0.25 µg/mL in H$_2$O) and doxorubicin plus PGA-**1** in case of U937 for 24, 48 and 72 hours. Apoptosis was analyzed by flow cytometry by determining the changes in cell forward/side scatter and through the determination of phosphatidylserine (PS) exposure and mitochondrial membrane potential (ΔΨm) loss with Annexin V-FITC and 3,3-dihexyloxacarbocyanine iodide (DiOC$_6$(3)), respectively. Necrotic cell death was distinguished from apoptotic using propidium iodide (PI) by co-incubation either with Annexin V-FITC or with DiOC$_6$(3). FL1 detector was used to analyze Annexin V-FITC binding or DiOC$_6$(3) accumulation (λexc = 488 nm; λem = 530 nm) and PI staining was followed by signal detector FL3 (λexc = 530 nm; λem = 617 nm). For adherent cells, firstly these were gently trypsinized and washed twice with cold PBS. Then, cells were resuspended in 1x binding buffer (10 mM Hepes/NaOH (pH 7.4) 140 mM NaCl, 2.5 mM CaCl$_2$) at a concentration of 1×10^6 cells/ mL. After transferring 100 µL of the cell solutions (1×10^5 cells) to a 5 mL culture tube two different staining protocols were followed: (i) 5 µL of Annexin V-FITC and 5 µL of PI (ready-to-use solutions from the Apoptosis detection kit) were added to the cell solutions. Cells were gently vortexed and incubated for 15 min at RT in the dark. (ii) 5 µL of 100 nM DiOC$_6$(3) in PBS were added to the solution and cells incubated for 30 min at 37 °C. Then 5 µL of PI (ready-to-use solutions from the Apoptosis detection kit) was also added and incubated for further 15 min at RT in the dark. The highly fluorescent population was considered viable cells, and the dull population represented apoptotic cells. Prior to flow cytometry analysis, 400 µL of 1x binding buffer were added in all cases to each tube.

Immunohistochemistry. Cardiomyocytes were fixed in 2 % paraformaldehyde (PFA). Immunohistochemistry was performed with antibodies against caspase-3 (1:100) and anti-α-actinine (Sacomeric) (1:800) followed by detection with secondary antibodies coupled to either Cyanine or FITC.

Statistical analysis. Data are expressed as mean ± standard error. Student t-tests were performed and means were considered statistically significant when p values less than 0,05 were obtained.

REFERENCES

(1) Martin, A. G.; Nguyen, J.; Wells, J. A.; Fearnhead, H. O. Apo cytochrome c inhibits caspases by preventing apoptosome formation. *Biochem. Biophys. Res. Comm.* **2004**, *319*, 944-950.

(2) Nencioni, A.; Grunebach, F.; Patrone, F.; Ballestrero, A.; Brossart, P. The proteasome and its inhibitors in immune regulation and immune disorders. *Critical Rev. Immunol.* **2006**, *26*, 487-497.

(3) Fischer, U.; Schulze-Osthoff, K. New approaches and therapeutics targeting apoptosis in disease. *Pharmacol. Rev.* **2005**, *57*, 187-215.

(4) Takemura, G.; Fujiwara, H. Morphological aspects of apoptosis in heart diseases. *J Cell Mol Med.* **2006**, *10*, 56-75.

(5) Mattson, M. P.; Kroemer, G. Mitochondria in cell death: novel targets for neuroprotection and cardioprotection. *Trends Mol Med.* **2003**, *9*, 196-205.

(6) Siegel, R. M. Caspases at the crossroads of immune-cell life and death. *Nat Rev Immunol.* **2006**, *6*, 308-317.

(7) Chai, J. J.; Du, C. Y.; Wu, J. W.; Kyin, S.; Wang, X. D. et al. Structural and biochemical basis of apoptotic activation by Smac/DIABLO. *Nature* **2000**, *406*, 855-862.

(8) Li, P.; Nijhawan, D.; Budihardjo, I.; Srinivasula, S. M.; Ahmad, M. et al. Cytochrome c and dATP-dependent formation of Apaf-1/caspase-9 complex initiates an apoptotic protease cascade. *Cell.* **1997**, *91*, 479-489.

(9) Schafer, Z. T.; Kornbluth, S. The apoptosome: physiological, developmental, and pathological modes of regulation. *Dev Cell.* **2006**, *10*, 549-561.

(10) Mochizuki, H.; Hayakawa, H.; Migita, M.; Shibata, M.; Tanaka, R. et al. An AAV-derived Apaf-1 dominant negative inhibitor prevents MPTP toxicity as antiapoptotic gene therapy for Parkinson's disease. *Proc Natl Acad Sci U S A.* **2001**, *98*, 10918-10923.

(11) Cao, G. D.; Xiao, M.; Sun, F. Y.; Xiao, X.; Pei, W. et al. Cloning of a novel Apaf-1-interacting protein: A potent suppressor of apoptosis and ischemic neuronal cell death. *Journal of Neuroscience* **2004**, *24*, 6189-6201.

(12) Malet, G.; Martín, A. G.; Orzáez, M.; Vicent, M. J.; Masip, I. et al. Small molecule inhibitors of Apaf-1-related caspase-3/-9 activation that control mitochondrial-dependent apoptosis. *Cell Death Differ.* **2006**, *13*, 1523-1532.

(13) Orzaez, M.; Mondragon, L.; Marzo, I.; Sanclimens, G.; Messeguer, A. et al. Conjugation of a novel Apaf-1 inhibitor to peptide-based cell-membrane transporters: Effective methods to improve inhibition of mitochondria-mediated apoptosis. *Peptides* **2007**, *28*, 958-968.

(14) Vicent, M. J.; Pérez-Payá, E. Poly-L-glutamic acid (PGA) Aided Inhibitors of Apoptotic Protease Activating Factor 1 (Apaf-1): An Antiapoptotic Polymeric Nanomedicine. *J. Med. Chem.* **2006**, *49*, 3763-3765.

(15) Tsujimoto, Y. Role of Bcl-2 family proteins in apoptosis: apoptosomes or mitochondria? *Genes to Cells* **1998**, *3*, 697-707.

(16) Chan, S. L.; Yu, V. C. Proteins of the bcl-2 family in apoptosis signalling: from mechanistic insights to therapeutic opportunities. *Clin Exp Pharmacol Physiol* **2004**, *31*, 119-128.

(17) Duncan, R. Drug Polymer Conjugates - Potential for Improved Chemotherapy. *Anti-Cancer Drugs* **1992**, *3*, 175-210.

(18) Lademann, U.; Cain, K.; Gyrd-Hansen, M.; Brown, D.; Peters, D. et al. Diarylurea compounds inhibit caspase activation by preventing the formation of the active 700-kilodalton apoptosome complex. *Mol. Cell. Biol.* **2003**, *23*, 7829-7837.

(19) Nguyen, J. T.; Wells, J. A. Direct activation of the apoptosis machinery as a mechanism to target cancer cells. *Proc Natl Acad Sci U S A.* **2003**, *100*, 7533-7538.

(20) Bras, M.; Queenan, B.; Susin, S. A. Programmed cell death via mitochondria: different modes of dying. *Biochemistry (Mosc).* **2005**, *70*, 231-239.

(21) Green, D. R. Apoptotic pathways: Ten minutes to dead. *Cell* **2005**, *121*, 671-674.

(22) Martinou, I.; Desagher, S.; Eskes, R.; Antonsson, B.; Andre, E. et al. The release of cytochrome c from mitochondria during apoptosis of NGF-deprived sympathetic neurons is a reversible event. *J Cell Biol.* **1999**, *144*, 883-889.

(23) Seye, C. I.; Knaapen, M. W. M.; Daret, D.; Desgranges, C.; Herman, A. G. et al. 7-ketocholesterol induces reversible cytochrome c release in smooth muscle cells in absence of mitochondrial swelling. *Cardiovascular Res.* **2004**, *64*, 144-153.

(24) Anversa, P.; Cheng, W.; Liu, Y.; Leri, A.; Redaelli, G. et al. Apoptosis and myocardial infarction. *Basic Res. Cardiol.* **1998**, *93*, 8-12.

(25) Itoh, G.; Tamura, J.; Suzuki, M.; Suzuki, Y.; Ikeda, H. et al. DNA fragmentation of human infarcted myocardial cells demonstrated by the nick end labeling method and DNA agarose gel electrophoresis. *Am. J. Pathol.* **1995**, *146*, 1325-1331.

(26) Schwarz, K.; Simonis, G.; Yu, X.; Wiedemann, S.; Strasser, R. H. Apoptosis at a distance: remote activation of caspase-3 occurs early after myocardial infarction. *Mol. Cell. Biochem.* **2006**, *281*, 45-54.

(27) Fliss, H.; Gattinger, D. Apoptosis in ischemic and reperfused rat myocardium. *Circ. Res.* **1996**, *79*, 949-956.

(28) Gottlieb, R. A.; Engler, R. L. Apoptosis in myocardial ischemia-reperfusion. *Ann N Y Acad Sci.* **1999**, *874*, 412-426.

(29) Wang, G. W.; Zhou, Z.; Klein, J. B.; Kang, Y. J. Inhibition of hypoxia/reoxygenation-induced apoptosis in metallothionein-overexpressing cardiomyocytes. *Am. J. Physiol. Heart Circ. Physiol.* **2001**, *280*, H2292-2299.

(30) Ferrari, R. Metabolic disturbances during myocardial ischemia and reperfusion. *Am. J. Cardiol.* **1995**, *76*, 17B-24B.

(31) Lucas, D. T.; Szweda, L. I. Declines in mitochondrial respiration during cardiac reperfusion: age-dependent inactivation of alpha-ketoglutarate dehydrogenase. *Proc Natl Acad Sci U S A.* **1999**, *96*, 6689-6693.

(32) Wencker, D.; Chandra, M.; Nguyen, K.; Miao, W. F.; Garantziotis, S. et al. A mechanistic role for cardiac myocyte apoptosis in heart failure. *J. Clin. Invest.* **2003**, *111*, 1497-1504.

(33) Hayakawa, Y.; Chandra, M.; Miao, W. F.; Shirani, J.; Brown, J. H. et al. Inhibition of cardiac myocyte apoptosis improves cardiac function and abolishes mortality in the peripartum cardiomyopathy of G alpha q transgenic mice. *Circulation* **2003**, *108*, 3036-3041.

(34) Masip, I.; Cortes, N.; Abad, M. J.; Guardiola, M.; Perez-Paya, E. et al. Design and synthesis of an optimized positional scanning library of peptoids: identification of novel multidrug resistance reversal agents. *Bioorg. Med. Chem.* **2005**, *13*, 1923-1929.

(35) Kijima, K.; Matsubara, H.; Murasawa, S.; Maruyama, K.; Mori, Y. et al. Mechanical stretch induces enhanced expression of angiotensin II receptor subtypes in neonatal rat cardiac myocytes. *Circ. Res.* **1996**, *79*, 887-897.

(36) Sgouras, D.; Duncan, R. Methods for the Evaluation of Biocompatibility of Soluble Synthetic-Polymers Which Have Potential for Bio-Medical Use .1. Use of the Tetrazolium-Based Colorimetric Assay (Mtt) as a Preliminary Screen for Evaluation of Invitro Cytotoxicity. *J. Mater. Sci.-Mater. Med.* **1990**, *1*, 61-68.